JOURNAL OF APPLIED ELECTROCHEMISTRY 24 (1994) 475–480

Coplanar interdigitated band electrodes for synthesis Part I: Ohmic loss evaluation

C. BELMONT

Department of Chemistry, University of Edinburgh, West Mains Road, Edinburgh EH9 3JJ, Great Britain

H. H. GIRAULT

Laboratoire d'Electrochimie, Département de Chimie, Ecole Polytechnique Fédérale de Lausanne, CH-1015 Lausanne, Switzerland

Received 3 March 1993; revised 2 June 1993

A new type of electrosynthesis cell consisting of coplanar interdigitated band electrodes is proposed. This approach permits minimization of the anode/cathode separation to a few hundred micrometres without hindering the hydrodynamics. In this paper, two analytical expressions are considered for the solution resistance between the bands. Results obtained for different geometries are compared to experimental data. It is shown that a substantial decrease in ohmic loss during synthesis can be achieved.

Nomenclature

C_{geom}	dimensionless constant related to the array geometry
C_{NaCl}	sodium chloride concentration (M)
e_{th}	electrode thickness (μm)
J	cell constant (cm^{-1})
l_b	length of exposed band
l_{eq}	equivalent length (mm)
n_b	total number of bands in the array
R_{array}	total resistance between the bands of an array (Ω)
R_{bu}	resistance between two bands of unit length (Ωm)
R_{th}	resistance associated with the electrode thickness (Ω)
$2V_0$	applied differential potential (V)
W_e	electrode band width (mm)
W_g	interelectrode band gap (mm)

Greek symbols

ϕ	potential (V)
Λ_{NaCl}	sodium chloride molar conductivity ($cm^2\,\Omega^{-1}\,mol^{-1}$)
ρ	resistivity (Ωm)

1. Introduction

The design of electrochemical reactors is a balance between the optimization of the mass transfer conditions and the minimization of the energy loss in Joule heating of the electrolyte. Many electrochemical cell geometries have been proposed including tank reactors, parallel plate cells, trickle towers, rotating and porous electrode cells [1, 2]. Figures of merit have been compared and substantial differences can be found [2, 3]. When the electrolysis is carried out in organic solvents, the resistance of the solution becomes an important criterion resulting in a large dissipation of energy. To minimize the ohmic loss, cells with small interelectrode distances have been designed such as the capillary gap cells and the pump cell [3]. The drawback of such approaches is the poor mass transfer conditions which result in an additional energy cost for the pumping of the solution through the cell.

In the present paper we propose another approach for the ohmic loss minimization based on microelectrode methodology. Microelectrodes have specific features such as the ability to work in very resistive media and steady state diffusional profiles and for these reasons have found many applications in electroanalytical chemistry, as recently reviewed [4–7]. An interesting aspect of microelectrode technology is the concept of interdigitated microband electrodes which is commonly used for the fabrication of conductivity sensors [8, 9] and amperometric detectors in liquid chromatography [10, 11]. Their performance and characteristics have been thoroughly investigated and the purpose of the present work is to apply this technology to electrosynthesis.

The experimental approach undertaken to produce large scale interdigitated band electrodes with a micro gap between electrodes is that of screen printing. This technique has already been used in the electrochemical sensor industry and geometric areas of up to 1 m^2 can easily be printed with a resolution of 50 μm for the edge definition.

In this publication two models for the determination of resistances between band electrodes are

0021-891X

considered and compared to experimental results. The models proposed are then used to determine the optimum band array geometry.

2. Theory

In order to derive an expression for the resistance between two bands, the system can be represented as shown in Fig. 1. Electrodes are defined by X_1 and X_2 or by $-X_1$ and $-X_2$, one electrode being polarized at zero and the other at $2V_0$. In an interdigitated device each band is shared with its two adjacent bands. Thus $(X_2 - X_1)$ represents half of the band width (W_e) and $2X_1$ is the interelectrode gap (W_g). The model is for infinite bands and therefore the phenomena occurring at the end of the bands are not considered.

Outside the 'submicron' (sub-micrometre) thick diffuse layers, the conductivity of a solution is assured by the movement of ionic species. Therefore for the estimation of a resistance, diffusion and convection forces can be ignored and the flux of charged species j is assumed to occur by migration only:

$$nFj = -\rho^{-1} \operatorname{grad} \phi \tag{1}$$

where ρ is the resistivity of the solution and ϕ the potential.

Assuming a steady state condition, the divergence of the flux is zero, thus,

$$\rho^{-1}\left(\frac{\partial^2\phi}{\partial X^2} + \frac{\partial^2\phi}{\partial Y^2}\right) = 0 \tag{2}$$

In these conditions the migration current, i, per unit length of electrode over the interval X_1 to X_2 is given by

$$i = \int_{X_1}^{X_2} \rho^{-1}\left(\frac{\partial\phi}{\partial Y}\right)_{Y=0} \mathrm{d}X \tag{3}$$

Similar equations have been solved by using conformal mapping techniques [12–15]. The corresponding change of variable is

$$x = \cosh u \cos v \tag{4}$$

$$y = \sinh u \sin v \tag{5}$$

where x and y are dimensionless variables defined by

$$x = X/X_1 \tag{6}$$

$$y = Y/X_1 \tag{7}$$

and v is the dimensionless potential,

$$v = \pi\phi/2V_0 \tag{8}$$

If Equation 4 is derived by x and Equation 5 by y, the main property of the transformation can easily be demonstrated. Thus,

$$\left(\frac{\partial u}{\partial x}\right)_{y=0,1<x<x_2} = \left(\frac{\partial v}{\partial y}\right)_{y=0,<x<x_2} \tag{9}$$

Hence Equation 3 can be integrated. So,

$$i = \frac{2V_0}{\pi\rho}\cosh^{-1}(X_2/X_1) \tag{10}$$

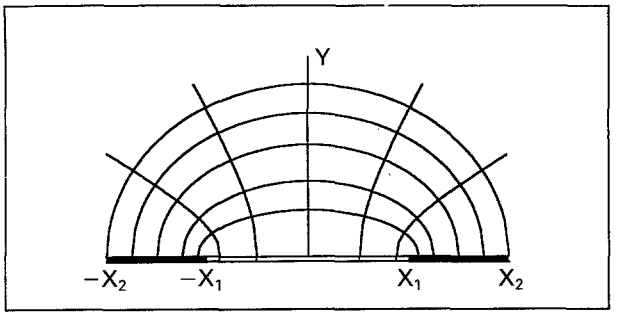

Fig. 1. Representation of the equipotential and flux lines between two parallel half band electrodes.

Equipotential lines shown in Fig. 1 are hyperbolae of equation

$$\frac{x^2}{\cos^2 v} - \frac{y^2}{\sin^2 v} = 1 \tag{11}$$

and the lines of flux between the two electrodes are ellipses given by

$$\frac{x^2}{\cosh^2 u} + \frac{y^2}{\sinh^2 u} = 1 \tag{12}$$

The current distribution along the electrode can be derived from Equation 10 by calculating the current for bands of infinitesimal width, δx:

$$i(x) = \frac{2V_0}{\pi\rho}\cosh^{-1}\left(\frac{x+\delta x}{x}\right) \tag{13}$$

Figure 2 illustrates this variation on the electrode taking $\delta x = 0.01$ and $2V_0/(\pi\rho) = 1$. As the current is related to the resistance of the solution ($2V_0 = Ri$), an expression can be derived for the resistance between two bands of unit length, $R_{bu}[\Omega \times m]$:

$$R_{bu} = \frac{\pi\rho}{\cosh^{-1}(X_1/X_2)} \tag{14}$$

For an array, the equivalent length l_{eq} is defined as the band length l_b times the number of gaps between electrodes, $(n_b - 1)$, as shown in Fig. 3. The total

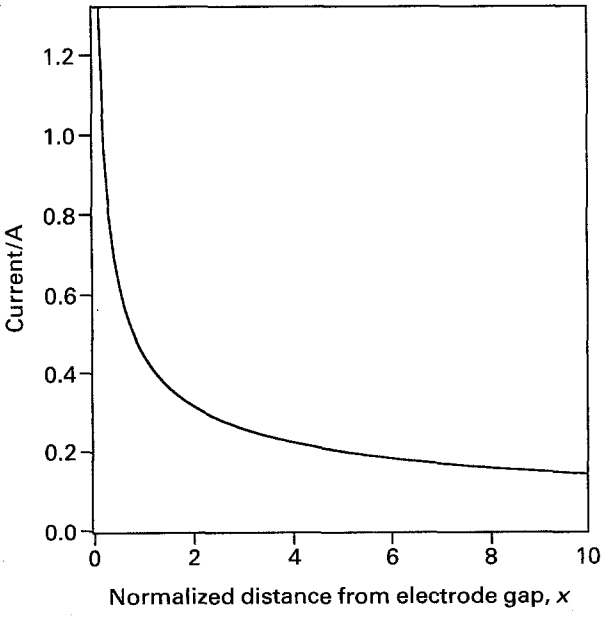

Fig. 2. Current distribution along the electrode.

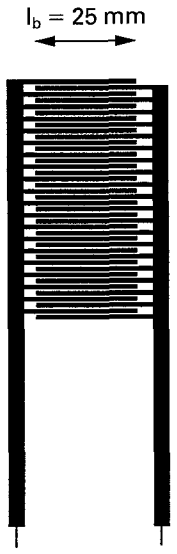

Fig. 3. Diagram of an interdigitated electrode (AG2) $n_b = 40$ and $l_{eq} = 975$ mm.

resistance R_{array} is then given by the following equation:

$$R_{array} = \frac{R_{bu}}{l_{eq}} = \frac{R_{bu}}{l_b \times (n_b - 1)} \quad (15)$$

The equivalent length varies from one array to another. To have comparable figures a dimensionless constant C_{geom} is introduced, depending only on the electrode width and the interelectrode gap,

$$C_{geom} = \frac{\pi}{\cosh^{-1}(W_e/W_g + 1)} \quad (16)$$

The constant C_{geom} corresponds to what is often referred to as the cell constant in conductivity measurements, multiplied by the equivalent length.

To obtain this solution, lines of flux and equipotential lines are assumed to be elliptical and hyperbolic, respectively, neglecting the fluxes which are very distant from the electrodes. The model developed by Aoki *et al.* [16] took them into account and they derived another expression for the current by solving the two dimensional equation, Equation 2, with the Schwarz–Christoffel transformation. From this the geometrical constant C'_{geom} is derived:

$$C'_{geom} = \pi/\ln(2.55(W_e/W_g + 1) - 0.19/(W_e/W_g + 1)^2) \quad (17)$$

Both these models have been used for the estimation of diffusional currents and have shown good correlation with experimental results [17].

3. Experimental details

Three different band arrays were made by screen printing silver ink (Johnson Matthey, UK) on PVC substrates. They all had the same electrode width, W_e, and band length l_b. Only the interelectrode gap, W_g and the number of bands n_b were changed. The geometrical parameters are shown in Table 1. They were then cured at 60° C for 24 h and the contacts were covered with an insulating varnish. The screen printer used was a manual bench top version (DEK 65, UK) for prototype production. Electrode thickness was determined by scanning electron microscopy (JEOL JSM 6300F). Impedance measurements were carried out with arrays placed vertically in quiescent aqueous solutions of sodium chloride, concentrations varying in the range 5×10^{-3} to 0.15 M. The equipment used for impedance measurements was a TFA2000 a.c. impedance analyser from Sycopel Scientific Ltd, UK. Measurements were carried out with an a.c. voltage of 10 mV. The resistance was extracted from the Nyquist plot at high frequencies and at zero imaginary impedance, i.e. when the system was purely resistive.

Table 1. Geometry of the interdigitated arrays

	n_b	W_g/mm	W_e/mm	l_b/mm
AG1	30	1 ± 0.1	1 ± 0.1	25 ± 1
AG2	40	0.5 ± 0.1	1 ± 0.1	25 ± 1
AG3	50	0.25 ± 0.05	1 ± 0.1	25 ± 1

4. Results and discussion

The values of the resistances measured for the three arrays (AG1, AG2 and AG3) in sodium chloride solutions of concentrations 5×10^{-3} to 0.15 M are shown in Table 2. The linear response between the resistance and the reciprocal of the concentration of sodium chloride is highlighted by Fig. 4. For an infinitely concentrated solution, the resistance is only due to the electrode and can be estimated at 1.5 Ω from the intercept values on the y-axis. The cell constant J can then be calculated from these data ($J = (R - 1.5)/\rho$, with $\rho = 1/\Lambda_{NaCl} \cdot C_{NaCl}$ and average $\Lambda_{NaCl} = 108\ cm^2\ \Omega^{-1}\ mol^{-1}$). In Table 2, it can be seen that the cell constants are very constant over the range of concentrations

Table 2. Theoretical and experimental data for different arrays

Array	*AG1*	*AG2*	*AG3*
$10^3 C_{NaCl}$/M		$R_{measured}/\Omega$	
5	45.75	30.55	23.50
10	23.30	15.75	12.00
25	10.70	7.65	6.00
50	6.05	4.35	3.55
100	3.65	3.10	2.65
150	3.05	2.70	2.30
$10^3 C_{NaCl}$/M		J/cm^{-1}	
5	0.0239	0.0157	0.0119
10	0.0235	0.0154	0.0113
25	0.0248	0.0166	0.0121
50	0.0246	0.0154	0.0111
100	0.0232	0.0173	0.0124
150	0.0251	0.0194	0.0130
Average value of J	0.0242	0.0166	0.0120
$C_{geom(exp)}$	1.74 ± 0.08	1.56 ± 0.07	1.47 ± 0.06
C_{geom}	2.38	1.78	1.23
C'_{geom}	1.94	1.55	1.23

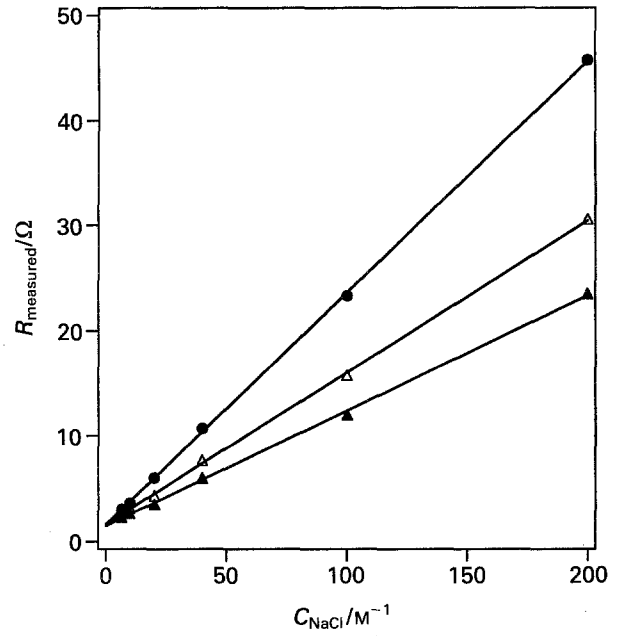

Fig. 4. The variation of the resistance with the reciprocal of the sodium chloride concentration. (●) AG1, (△) AG2 and (▲) AG3.

studied. Their average is used for the determination of the geometrical constant ($C_{geom(exp)} = J \times l_{eq}$). Experimental and theoretical geometrical constants are compared in Table 2. They have the same order of magnitude as can be seen in Fig. 5. Although the first model which assumes elliptical current lines presents good correlation for small interelectrode gaps, the second model derived using the Schwarz–Christoffel transformation seems to fit better with the experimental data. Nevertheless, it is worthwhile to note that for large interelectrode gaps the two models are able to estimate the ohmic losses, and therefore the discussion which follows gives a conservative value of the ohmic loss savings which can be achieved by the approach. It is also worthwhile to note that in the models developed

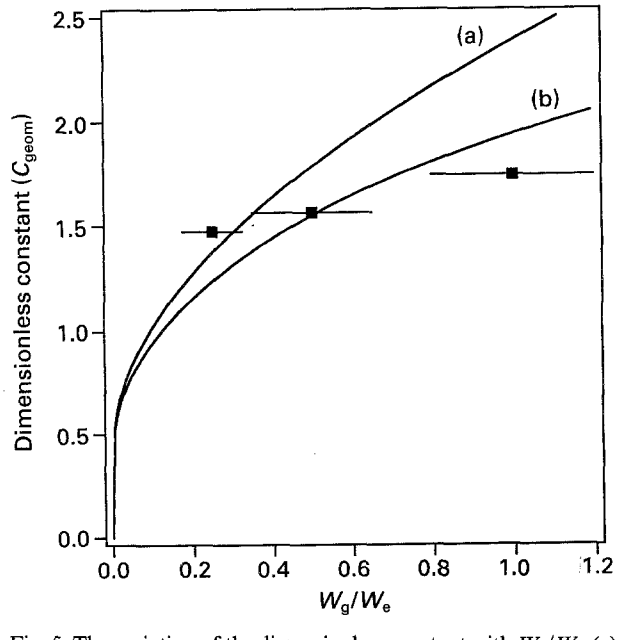

Fig. 5. The variation of the dimensionless constant with W_g/W_e: (a) from Equation 16 and (b) from Equation 17. (■) Experimental values.

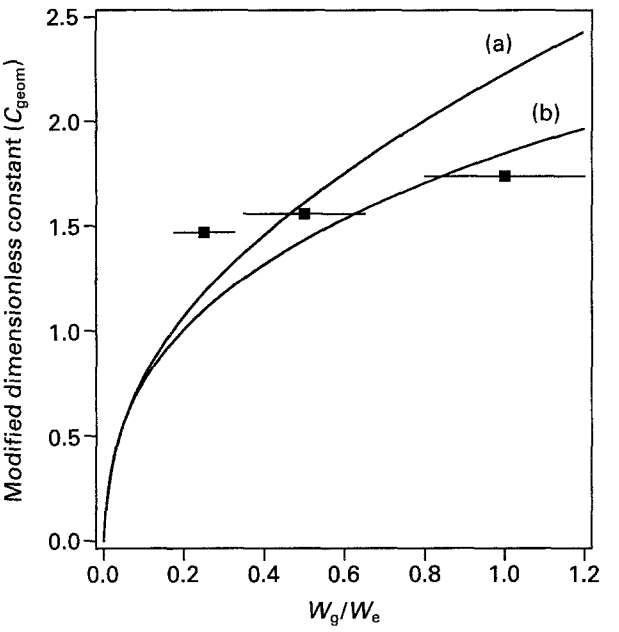

Fig. 6. The variation of the modified dimensionless constant with W_g/W_e, for a 25 μm thick electrode: (a) from Equation 16 and (b) from Equation 17.

previously, the thickness of the electrode was not taken into account. The resistance between two parallel plates of surface $e_{th} \times l_{eq}$ and separated by W_g is given by:

$$R_{th} = \frac{\rho W_g}{e_{th} l_{eq}} \tag{18}$$

The two models can be modified so that the total resistance is formulated for a system with two resistances in parallel (resistance above the electrodes and resistance between the electrodes). The thickness of the electrodes was found to be 25 μm with a standard deviation of 5 μm. The corresponding geometrical constants do not vary dramatically but when compared with the experimental data in Fig. 6, the first model appears to be the most appropriate one.

To demonstrate that ohmic losses can be reduced by using band arrays, the cell constant ($J = R/\rho$) is calculated for the different arrays and compared with the cell constant of a parallel cell. In the case of the FMO1 cell from ICI ($16 \times 4\,cm^2 \times 0.3\,cm$) the geometrical constant is

$$J = \frac{0.3}{16 \times 4} = 0.0047\,cm^{-1}$$

If a plate is replaced by a band array of the same area ($16 \times 4\,cm^2$) the cell constant can be determined from Equations 16 and 17. Figure 7 shows their variation with the electrode and the gap widths. It is clear that the closer the band, the smaller the resistance. For 250 μm interelectrode gaps, ohmic losses can be reduced by 50% in comparison to what should be obtainable with the ICI cell. The graphs also show that there is an optimum electrode width $W_{e,opt}$ for each interelectrode spacing for which the geometrical constant is at a minimum. The relationships between the two sizes are purely linear as shown in Fig. 8. The proportional factors are different for the two

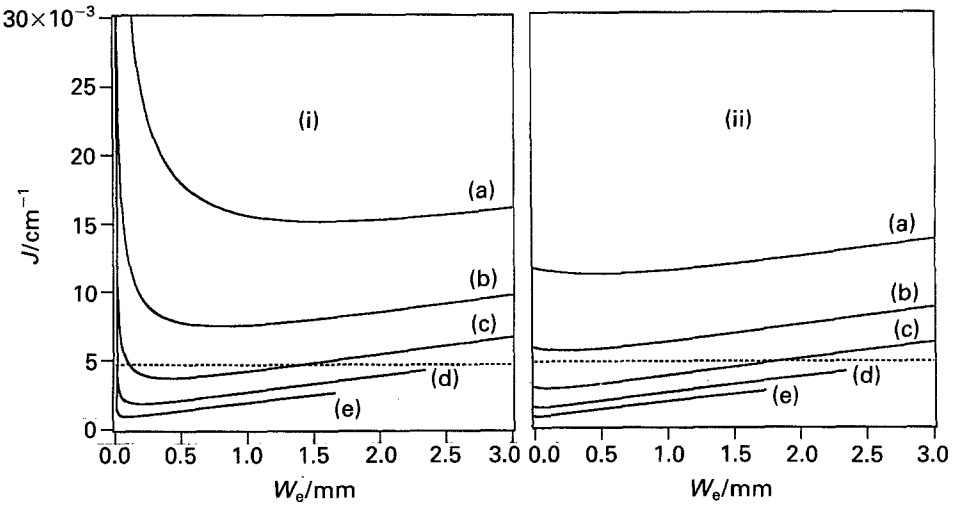

Fig. 7. The variation of the geometrical constant with the electrode width for different band gaps: (i) from Equation 16, (ii) from Equation 17 (a) $W_g = 2$ mm, (b) $W_g = 1$ mm, (c) $W_g = 0.5$ mm, (d) $W_g = 0.25$ mm, (e) $W_g = 0.125$ mm and (- - -) ICI FM01 geometrical constant.

models, but considering that for the second model an increase in the electrode width has very little effect, the band width should be such that

$$W_e = 0.8W_g$$

However, in designing interdigitated electrode systems, the ohmic loss within the band electrode itself must be considered, especially if the electrode material is not a good conductor. In the case of screen printed metal this is not a real problem, however, when fabricating carbon band electrodes, a compromise must be made between the reduction of ohmic loss in the solution and the increase in the ohmic loss in the electrode.

5. Conclusion

It is clear that the proposed electrosynthesis cell with interdigitated coplanar anode and cathode can be built so as to minimize the ohmic loss compared to a conventional parallel plate cell. The present work shows that for an interelectrode gap of 250 μm and an electrode width of 200 μm, the ohmic loss is reduced by as much as 50% in comparison to a parallel plate of equivalent total area.

This could be very useful in organic media such as DMF. This work is part of a research program for the development of batch electrolysis with disposable electrodes. Applications to different organic syntheses will be published subsequently.

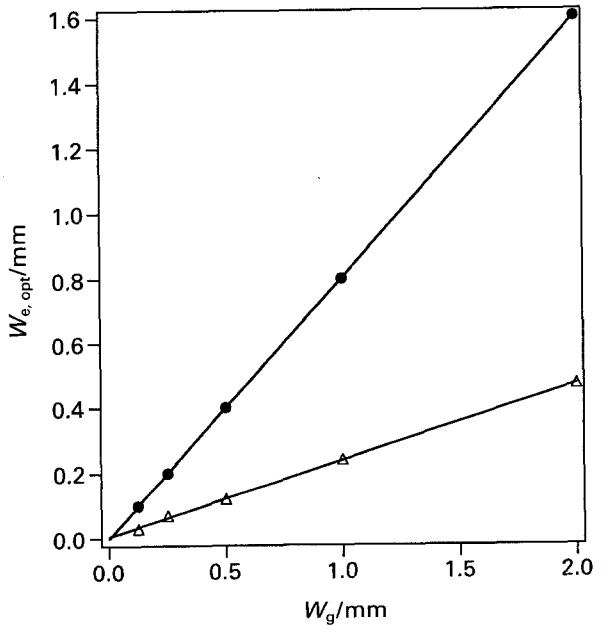

Fig. 8. The variation of the optimal electrode width $W_{e,opt}$ with the band gap: (●) from Equation 16 and (△) from Equation 17.

Acknowledgements

The authors are extremely grateful to Electricité de France Direction des Recherches who financed the project. One of us (CB) thanks this organization for a postgraduate fellowship as well as EPFL for a visiting scholarship. The authors also wish to thank ICI Electrochemical Technology Group for the loan of a FM cell.

References

[1] J. D. Genders and D. Pletcher, 'Electrosynthesis from Laboratory, to Pilot, to Production', The Electrosynthesis Company Inc., New York (1990).
[2] D. Pletcher and F. C. Walsh, 'Industrial Electrochemistry', Chapman & Hall, New York (1990).
[3] F. Coeuret and A. Storck, 'Eléments de Génie Electrochimique', Technique et Documentation, Lavoisier, Paris (1984).
[4] R. M. Wightman, *Anal. Chem.* **53** (1981) 1125R.
[5] M. I. Montenegro, M. A. Queiros and J. L. Daschbar (Eds.), *Microelectrodes: Theory and Applications*, NATO ASI series, **197** (1991).
[6] R. M. Whightman and D. O. Wipf, *Electroanal. Chem.* **15** (1989) 267.
[7] M. Fleischman, S. Pons, D. R. Rolison and P. P. Schmidt, 'Ultramicroelectrodes', Datatech Systems, Morganton, NC (1987).
[8] K. R. Wehmeyer, M. R. Deakin and R. M. Wightman, *Anal. Chem.* **57** (1985) 1913.
[9] A. J. Bard, J. A. Crayston, G. P. Kittlesen, T. V. Shea and M. S. Wrighton, *ibid.* **58** (1986) 2321.
[10] K. Aoki, K. Tokuda and H. Matsuda, *J. Electroanal. Chem.* **217** (1987) 33.
[11] J. L. Anderson, K. K. Whiten, J. D. Brewster, T. S. Ou and W. K. Nonidez, *Anal. Chem.* **57** (1985) 1366.

[12] H. S. Carlsaw and J. C. Jaeger, 'Conduction of Heat in Solids', Oxford University Press, London (1959).
[13] A. Angot, 'Compléments de Mathématiques à l'usage de l'Electrotechnique et des Télécommunications', Editions de la Revue Optique, Paris (1957).
[14] B. Fosset, C. A. Amatore, J. E. Bartelt, A. C. Michael and R. M. Wightman, *Anal. Chem.* **63** (1991) 306.
[15] B. J. Seddon, H. H. Girault and M. J. Eddowes, *J. Electroanal. Chem.* **266** (1989) 227.
[16] K. Aoki, M. Morita, O. Niwa and H. Tabei, *ibid.* **256** (1988) 269.
[17] B. J. Seddon, PhD thesis, University of Edinburgh, UK (1989).